

Frontiers in Scientific Research and Technology

Online ISSN: 2682-2970
Print ISSN: 2682-2962
http://fsrt.journals.ekb.eg

FSRT J 12 (2025) 105 - 116

10.21608/fsrt.2025.418121.1177

Enhancing the performance of Polysulfone nanofiltration membrane by inclusion of salicylic acid as a hydrophilic modifier in the support layer

Sami Mazhar Y. Hassan ^{a,*}, Abdel-hameed Mostafa El-Aassar ^b, Zeinab Mohamed Anwar ^a, Manar Sobaih Bayoumi ^a, Mohamed E. A. Ali ^b

- ^a Chemistry Department, Faculty of Science, Suez Canal University, Ismailia, Egypt.
- ^b Egypt Desalination Research Center of Excellence (EDRC), Hydro-geochemistry Department, Desert Research Center (DRC), Cairo, 11753, Egypt.

ARTICLE INFO

Article history:
Received 8 September 2025
Received in revised form 30 October 2025
Accepted 2 November 2025
Available online 12 November 2025

Keywords

PVP, SA, NF, hydrophilicity, TFC

ABSTRACT

Many researchers have shown that improving the hydrophilicity of the membrane will reduce the membrane fouling and enhance the permeation flux. Accordingly, this paper examines the effect of incorporating Salicylic acid (SA) in Polysulfone (PSF) substrate layers of thin film composite (TFC) nanofiltration (NF) membranes onto the morphology, hydrophilicity, permeation, and salt retention properties. For this purpose, SA was blended at different weight ratios into the PSF/ Polyvinyl pyrolidone (PVP) casting solution to improve the hydrophilic and permeation properties. TFC membranes were fabricated by coating the PSF substrates with Polyamide (PA) thin films. The effects of PSF, PVP and SA dosages in the casting solutions on the membrane flux and rejection were studied. Samples of the fabricated membranes were characterized by X-Ray Diffraction (XRD) ,Scanning Electron Microscope (SEM), Fourier Transform Infrared Spectroscopy (FTIR), Water contact angle measurement, Brunauer Emmet Teller (BET) and Dynamic Mechanical Analysis (DMA). The results exhibited an improvement in the hydrophilicity and mechanical properties with an increase in the surface area of the acid-modified membranes. The fabricated membranes were applied to remove salts from water. Permeate flux and Na₂SO₄ rejection of the pure PSF membrane were 15 L/m²h and 77.7%, whereas for PSF/SA were 29.6 L/m²h and 92.2 % at 5 bar pressure. As a conclusion, the addition of SA gives rise to membranes with higher permeate flux and salt rejection than the pure membrane. Also, the substrate layer fabricated from 16% PSF and 0.35% PVP with 0.35 % SA gives the best possible performance for the obtained membrane.

1. Introduction

Membrane-depended separation technologies have manifested their unparalleled power for the seawater desalination and remediation of manufacturing wastewater, which make them one of the prospective solutions for the present water crisis [1,2]. Separation methods by membranes can be assorted as microfiltration (MF), ultrafiltration (UF), nanofiltration (NF), and reverse osmosis (RO). Membranes are in general assorted by pore size, structure and mechanism of separation [3].

Among diverse membrane processes, NF process characterizes by low required pressures, high fluxes, high rejections of multivalent salts and low operation costs giving rise to be used in numerous separation and treatment processes such as treatment of water with a low content of ion (e.g., surface water and fresh ground water)

with a fundamental objective of water softening (multivalent ions removal), wastewater treatment, removal of color and micro pollutants, chemical and biological oxygen demand reduction (COD and BOD respectively), pharmaceutical and biochemical industries. Nanofiltration is susceptible to fouling as with any other membrane process. Fouling occurs by adsorption of solute particles comprising: colloidal, organic and biofouling, in addition to salt precipitation either on top of membrane or inside its pores. As fouling makes membrane efficiency worse and existence period shorter, therefore it is necessary to explore methods to promote antifouling NF membranes [4]. Numerous studies have focused recently on decreasing the membrane fouling. According to studies, Fouling can be reduced by the following methods: (1) blending PSF with hydrophilic nanoparticles, (2) blending with hydrophilic polymers, (3) adding monomers or functional groups and coating with hydrophilic polymers [5]. Multilayered TFC polyamide membrane is one more significant evolution in the membrane science including (1) upper ultra-thin film PA stratum (0.1–1µm) established

^{*} Corresponding author at Suez Canal University E-mail addresses: smy8696@gmail.com (Sami Mazhar Y. Hassan)

through IP of amine or diamine monomers (like mdiamine (MPD), Piperazine phenylene triethanolamine (TEOA) in aqueous phase and acyl chloride monomers (like TMC or isophethaloyl chloride (IPC) in organic phase, (2) In between PSF porous substrate and (3) non-woven polyester texture in the undermost. Those TFC membranes are types of nanofiltration membranes which largely utilized in the removal of salts and organics from water [6]. In TFC membranes, the upper-thin film and the support underlayer can be separately amended regarding structure, stability, and efficiency [7]. To investigate the effect of a support layer on the formation of NF membrane, many studies have been done in the past recent years to examine the effect of changing the support layer properties on the properties of ultra-thin PA selective layer [8-10]. It is believed that the morphology and the efficiency (i.e. permeability and rejection) of a TFC membrane may be altered with the use of different substrate properties [8,11,12]. Researchers have executed numerous studies to examine the influences of polymer dosage and additives on the performance of the porous support layer. The membrane porosity is influenced greatly by the dosage of polymer in the casting solution [13]. Increasing the polymer concentration results in a lower porosity as a result of increasing the solution viscosity, thus reducing transmission rates and slowing the demixing process [14]. Mohamed E.A. Ali et al. examined the impact of doping appointed organic acids in PSF casting solution onto the efficiency of NF membranes contains a thin film composed from m-phenylenediamine and TMC. The acidmodified PSF/TFC membranes displayed an increase in both of salt rejection and water flux with respect to the primal membrane. Water flux and salt rejection (%) of the primal membrane was 7.6 L/m²h and 65.4 %, whereas PSF/methacrylic acid, PSF/tartaric acid, and PSF/lactic acid were 16.8, 18.5 and 20.2 L/m²h and 88, 88.2 and 94.1%, respectively [15]. N. Ghaemi et al. concluded that incorporating of some organic acids (ascorbic, citric, and maleic acid) in the casting solution of NF membrane influenced the membrane morphology and improved the membrane performance [16]. A. Akbari et al. revealed that the addition of lactic acid, maleic acid, and citric acid in the casting solution of TFC NF membranes resulted in an enhancement in the water flux whilst the effect on salt rejection was low [17]. They attributed this to improving the hydrophilicity and porosity of the membranes due to the carboxylic and hydroxyl functional groups of the organic acids [18]. The present work aims to investigate using SA for enhancement of the hydrophilicity and permeability of PSF/TFC nanofiltration membranes in the presence of PVP as a pore forming agent. The impacts of PSF, PVP, and SA concentrations in the casting solutions on the membrane efficiency were studied. To the best of our knowledge, no report has been published regarding studying SA effects on PSF nanofiltration performance and membrane structure.

2. Materials & methods

2.1 Materials

Polysulfone granule (PSF, Udel P 3500 LCD MP7, Mn = 22,000); was used as the membrane based polymer. Salicylic acid (SA) was used as an additive (M.w. 138, loba Chemie) additive. Polyvinyl pyrolidone (PVP) to form pores (M.w. 40,000, Alpha Chemika). 1, 3, 5-Benzene-tricarbonvl trichloride (TMC) (> 98%), Piperazine anhydrous (PIP) (Merck, Germany) were utilized in establishing the PA thin film. N, N-Dimethylformamide (DMF) (99.9 %, CARLO ERBA) was used as a solvent for PSf and PVP. N-hexane was analytical grade and used as a solvent for TMC. Sodium sulfate (Na₂SO₄, 99.5 %), Sodium chloride (NaCl, 99%, LIVE CHEM), Magnesium chloride (ALDRICH) and Calcium Sulphate (CaSO₄) (98.5 %, Chemie-Pure) salts were used for preparation of the feed solutions. Chemical structures of PSf/ PVP and SA are illustrated in Fig. 1.

$$\begin{bmatrix} CH_3 & O & O & O \\ CH_3 & O & O & O \end{bmatrix}_n$$
(a)

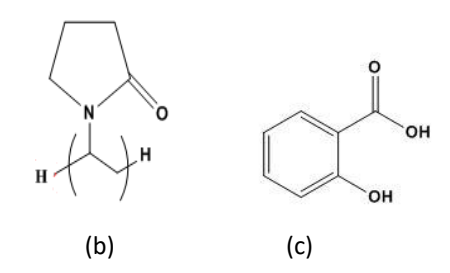


Fig. 1. Chemical structures of (a) PSF, (b) PVP and (c) SA.

2.2 Fabrication of PA/TFC membranes

NF membranes of PSF substrates with an asymmetric flat sheet structure were created using the phase inversion method. Table 1 presents the casting solution formulations. To prepare the casting solution, specific amounts of PSF, PVP and SA were dissolved in a solvent of DMF under vigorous stirring for 12 h at 70 °C until a homogeneous

solution was obtained. PVP and/or SA was first dissolved then PSF is added. To remove the air bubbles formed in the solution during its preparation (degassing), the dope solution was kept static for 4 h at room temperature (RT). Then, the prepared solution was casted without evaporation on a polyester non-woven fabric. Subsequently, the coated support was submerged in a

water bath for water-solvent exchange and as a result the polymer is precipitated. The fabricated membrane was then stored in a distilled water for a day to eject most of the solvent and water-soluble constituents. The TFC membrane was fabricated by dipping the prepared membrane support layer in 1.0 wt. % PIP aqueous solution for 2 min, then a tissue paper was used for removing of the surplus solution on the surface. The PSF support layer satiated with PIP was thereafter immersed for 60 seconds into an organic solution of 0.15 wt. % TMC/ hexane leading to the formation of a PA thin-film. The synthesized TFC

membranes were cured at 60 °C for 15 minutes, then washed thoroughly with distilled water for removing the surplus amine. Afterwards, the fabricated membranes were then kept in distilled water at room temperature until further use. A schematic representation of the PSF-SA composite membrane and a graphical description of the TFC membrane preparation process are shown in Fig. 2 and 3 respectively.

Table 1.	Polymer	doped	solution	composition

Factor	substrate	PSF (g)	PVP (g)	SAc (g)	DMF (ml)
PSF concentration	TFC14, TFC16, TFC18, TFC20 (Pristine)	14,16,18,20			86, 84 , 82, 80
PVP concentration	0.08 wt. % PVP/TFC, 0.18 PVP/TFC ,0.35 wt. % PVP/TFC, 0.7 wt. % PVP/TFC	16	0.08, 0.17, 0.35, 0.70	_	84
SA concentration	0.5 SAc/TFC, 1.1 SAc/TFC 2.2 SAc/TFC , 4.4 SAc/TFC	16	0.35	0.08, 0.17, 0.35, 0.70	84

Fig. 2. Schematic representation of the PSF-SA membrane fabrication process by in-situ cross-linking and blending.

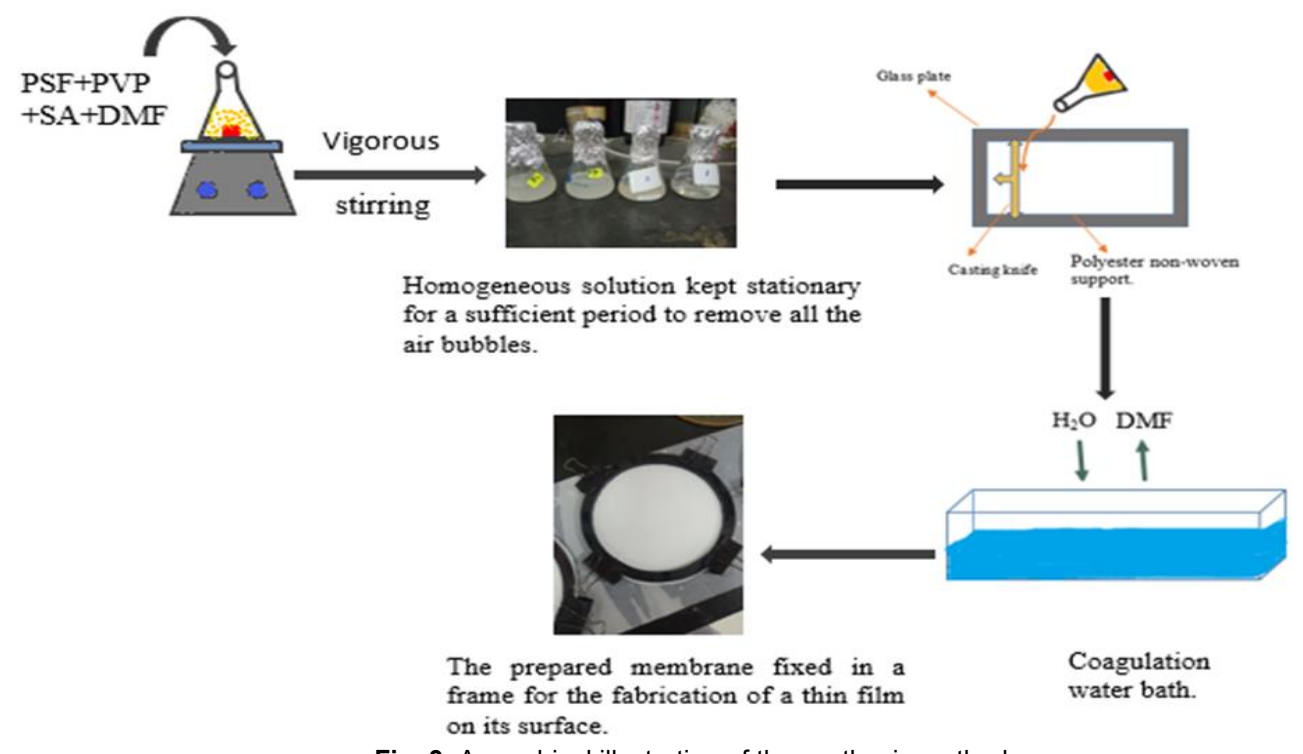


Fig. 3. A graphical illustration of the synthesis method.

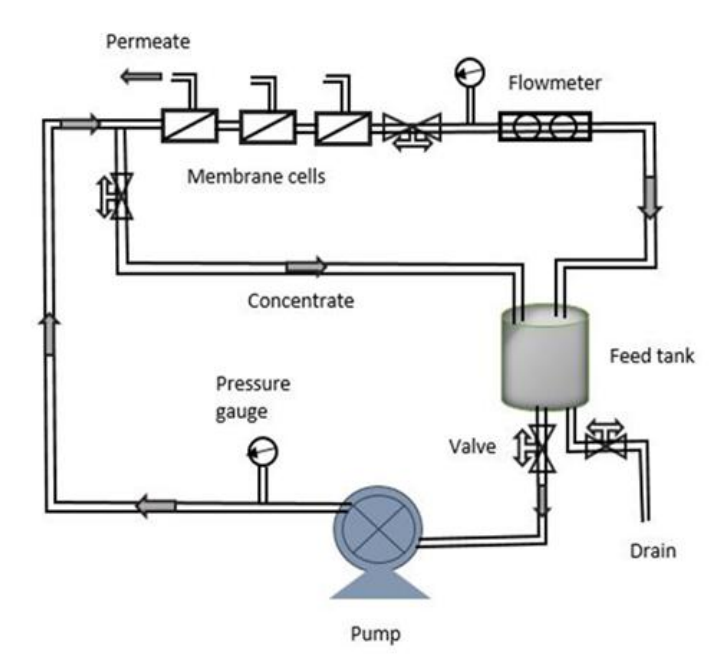
2.3 Membranes characterization

SEM (QUANTA, FEG 250) was utilized to depict the morphology of surface and cross-section of the synthesized membrane. FTIR (THERMO NICLOT, 50) was used to define the functional groups at a resolution between 4000 and 400 cm⁻¹. A contact angle analyzer (KRUSS, model DSA) was used to evaluate the hydrophilicity of the membranes surface. The XRD analysis was used for more confirmation to the presence of SA in the fabricated membranes. BET analyzer (Belsorp Mini X-Microtrac, Japan) was utilized to measure membrane surface area and pore size. A mechanical testing system DMA Q800 V21.1 Build 51 Module DMA Control Force was applied to measure the mechanical properties of the fabricated membranes including Tensile Strength (TS) and percent elongation.

2.4 Porosity and wettability study

The porosity of PSF membranes was measured using the gravimetric method. The method described by the literature [19] was followed in carrying out this test. Briefly, a specific area of the membranes was submerged in distilled water for a day. The wet weight was measured directly after taking out the membrane samples from water and wiping surplus water from the membrane surface by a tissue paper. After taking the weight, the membranes were left to dry at the atmospheric temperature for 24 h, and the weight was taken again. The porosity of membrane (£), was estimated by the next equation [19,20]:

$$\varepsilon$$
 (%) = $\frac{(w_w - w_d)/\rho_w}{(w_w - w_d)/\rho_w + w_d/\rho_p} \times 100$ (1)



(a) Schematic diagram

where w_w and w_d are the weights of wet and dry membranes (g), respectively. ρ_w is the pure water density while ρ_p is the polymer density. Similarly, the water Uptake capacity was evaluated by the next formula [19,20]:

Water Uptake (%) =
$$\frac{W_w - W_d}{W_w} \times 100$$
 (2)

2.5 Permeation flux and salt rejection

Across flow filtration system was utilized to implement the permeation test as shown in Fig. 4 with an effective membrane area of 50 cm². The prepared membranes were put in their specified place inside apparatus cells. Before proceeding of the experiment, a fixed pressure of 5 bar was applied on the membrane sample for half an hour with distilled water to get a steady permeate flux. For studying the membrane performance, a feed solution of 2500 ppm Na₂SO₄ salt was used. The permeate flux was calculated by Eq. (3): [21]

$$J = \frac{V}{Ax} \tag{3}$$

Where J is the measured permeate flux $(L/m^2 h)$, V is the volume of collected permeate solution (L), t = is the permeation time (h), A is the membrane effective area (m^2) . The salt rejection (R) value was calculated using Eq. (4):

$$R = \left(1 - \frac{\mathsf{Cp}}{cf}\right) \times 100 \tag{4}$$

Where C_p is permeate concentration and C_f is the feed concentration (mg/L). Salt concentration in aqueous solution was measured by a conductivity meter.



(b) Testing device

Fig. 4. Schematic diagram (a) and testing device (b) of the cross-flow unit used in this study.

3. Results and discussions

3.1 Membranes characterization

3.1.1 X-Ray Diffraction

Fig. 5 displays the XRD patterns of PSF/PVP membranes and PSF/PVP composite membranes blended with SA. As reported in a previous works for the literatures [4,5,22-25], the three peaks of high intensity in the XRD spectrum identified at 2θ angles of 18° , 23° and 26° are corresponding to the PSF/PVP matrix. As displayed in Fig. 5, the intensity of diffraction peaks in the PSF/SA XRD pattern has decreased which indicates an amorphous phase and a decrease in the crystallinity which may be due to disrupting the PSF molecule, interaction by the steric and repulsive effects of SA molecules [26]. The very small amount (0.35 wt.) of SA was considered to be the main factor for the peaks of SA which was not revealed in the PSf diffraction pattern as reported earlier [6].

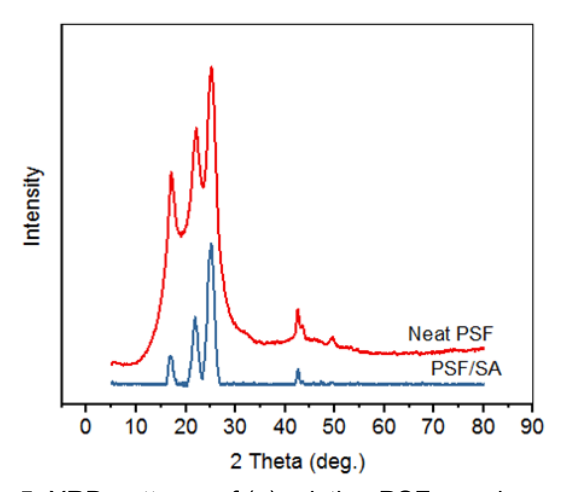


Fig. 5. XRD patterns of (a) pristine PSF membrane and (b) SA modified PSF membrane.

3.1.2 Fourier Transform Infrared

The FT-IR spectra of salicylic acid is presented in Fig. 6A. As displayed in the FT-IR spectrum of SA, distinctive vibrational peaks at wavenumbers 3233 cm⁻¹ and 2993-2848 cm⁻¹ were attributed to OH and C-H stretching, respectively. IR peaks located at 1605-1662 cm⁻¹ were distinctive to the C=O (COO-) asymmetric stretching. IR peaks existed at 1434-1475 cm⁻¹ were characteristic to the C-C stretching. IR peak defined at 1324 cm⁻¹ was attributed to the O-H (phenolic) bending. IR peaks presented at 1290 cm⁻¹ and 1141-1241 cm⁻¹, respectively were related to the COO- (C-O) stretching and C-OH (phenolic) stretching. (=C-H) bending was distinctive to the vibrational peaks manifested at 648-748 cm⁻¹. The literature data [27] was used to support the identified FT-IR data of SA. Fig.6B displays the IR spectrum of PSF membrane support layer in which characteristic peaks appear at wave numbers 692 cm⁻¹, 840 cm⁻¹, 1013 cm⁻¹, 1102 cm⁻¹, 1154 cm⁻¹, 1241 cm⁻¹ ¹, 1304 cm⁻¹, 1492 cm⁻¹, 1583 cm⁻¹ and 2966 cm⁻¹ are belonged to the aromatic C-H bending, S-O-C stretching, symmetric stretching vibration of diphenyl ether groups (C-O-C stretching), symmetric stretching of sulfonate groups (S=O), symmetric SO₂ stretching vibration, C-O-C asymmetric stretching vibration of the aryl-O-aryl group, C-SO₂-C asymmetric stretching vibration, C-H symmetric stretching vibration of CH3-C-CH₃, C=C aromatic benzene ring stretching and C-H aliphatic chain stretch, respectively [16,28-32]. The peak observed at 1678 cm⁻¹ in the FTIR analysis of the modified membranes (membranes with SA content) corresponds to the stretching of C=O groups of PVP molecules which remained in the membrane texture or the PSF casting solution without removing by water at the immersion precipitation procedure. In the IR spectrum of PSF/PVP membranes prepared by N. Ghaemi and Febriasari with co-workers [16,33], a new absorption peak manifested at 1639- 1660 cm⁻¹. They attributed the appearance of this peak to the part of PVP which did not leach out by water and remained inside the polymeric structure. All the TFC membranes (Fig. 6C) displayed additional characteristic new broad band manifested at 3400-3431 cm⁻¹ which could be attributed to the stretching vibrations of C-H and N-H of amide or could be characteristic to the -COOH groups of the PA thin film. The partial hydrolysis of the acyl chloride unit of TMC is the reason for the appearance of carboxylic acid functional groups. The intensity of this band increased in the IR spectrum of the SA modified membrane which may be related to the carboxylic group of SA. Also the characteristic band at 1625 cm⁻¹ is assigned to the stretching vibration of C=O in the active polyamide layer formed on the support membranes [16,34,15].

3.1.3 Scanning Electron Microscope

SEM was utilized to depict the cross-sectional and surface structure of the PSF membranes both before and after modification (Fig. 7). As demonstrated in the surface images, the ultrafiltration membranes surface (Fig.7a: c) was even and sleek, whereas the TFC membrane surface (Fig.7d) was uneven. The changes in the surface shape between TFC and pristine membranes confirm that the PA active layer had been formed successfully on top of the PSF substrate. The surface of TFC membranes appeared in a typical "globular-like nodular" morphology (Fig.7d). The SEM images displayed that the inclusion of SA in the PSF casting solution leads to a spongy-like sub-layer and a more porous surface of the substrate layer, which may be due to the reaction of SA with either the PSF chains or the solvent in the casting solution. Hydrogen bonds can be formed between hydrogen atoms of hydroxyl or carboxyl groups of SA acid and the oxygen atoms of PSF chains and the solvent which may lead to the migration of more PVP molecules to the surface and be leached out by water. As a result, the free space between the polymer chains will decrease and subsequently the solvent-water (non-solvent) replacement rate will decrease giving rise to membranes with more compact and less porous sub-layer. The rise in the surface porosity of the modified membranes can be because of the rise in the water inflow due to the acid hydrophilicity despite of the depression in the solvent (DMF) outflow. This observation was in agreement with a previous work of the literature [15].

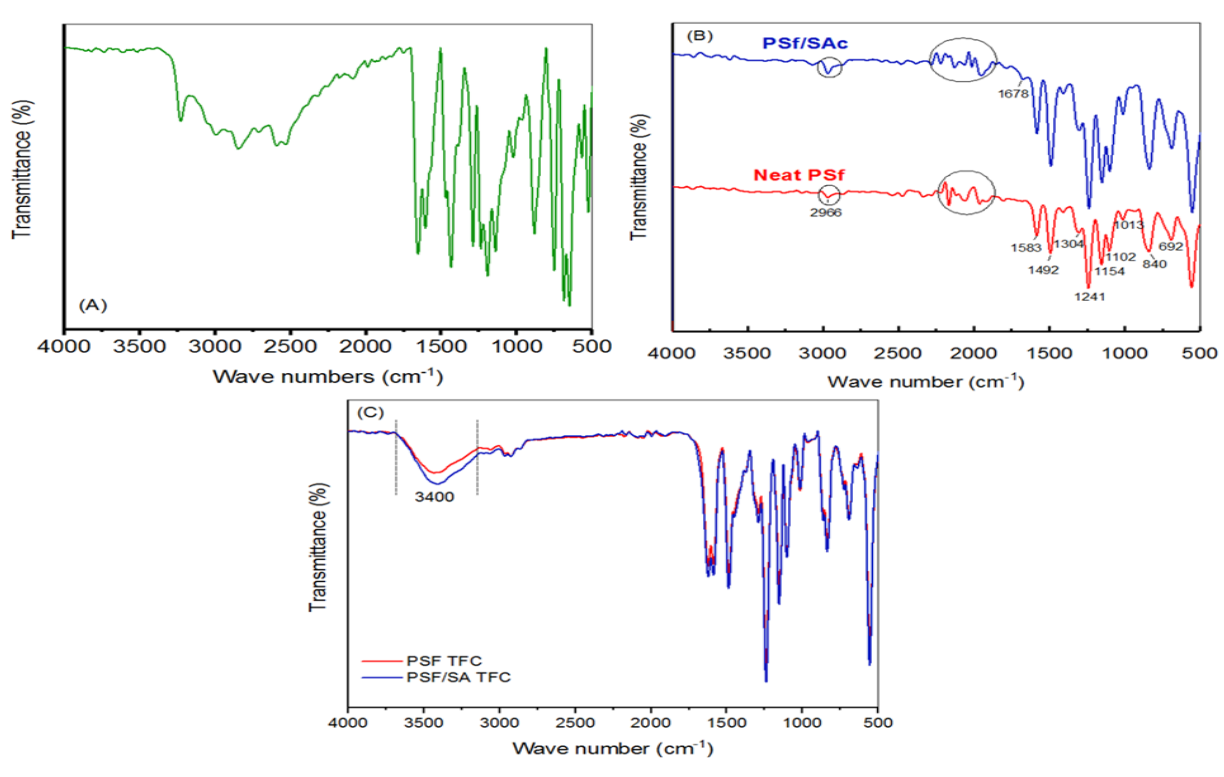


Fig. 6. FTIR spectra of (A) SA, (B) the pristine PSF and acid-modified PSF membrane and (C) TFC membranes.

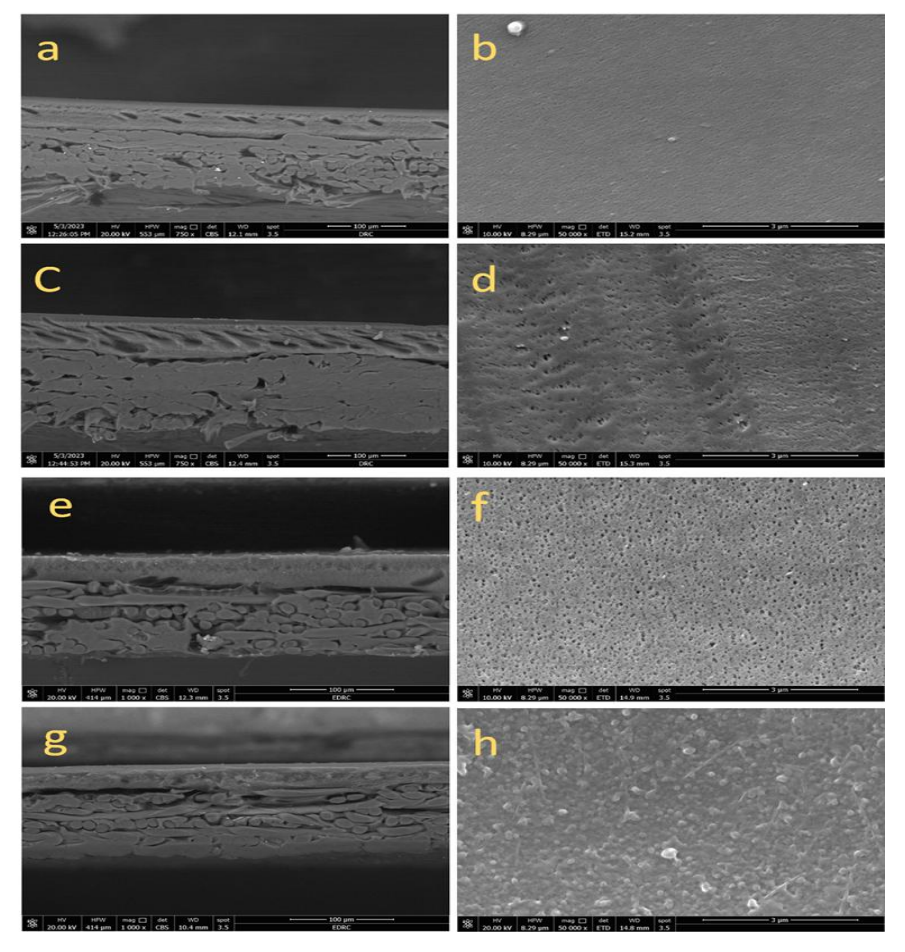


Fig. 7. SEM images of the cross sections (a,c,e and g) and surfaces (b,d,f and h) of membrane samples: (a and b) Neat PSF UF membrane, (c and d) PSF/PVP UF membrane, (e and f) PSF/SA (0.35 wt.%) UF membrane and (g and h) PSF/SA TFC membrane.

3.1.4 Contact angle and porosity characterization

Fig. 8 presents the water uptake, porosity and water contact angle (WCA) measured values of the neat and modified membranes. The hydrophilicity of the acid-modified membranes is expected to increase due to the existence of hydrophilic –OH and -COOH groups. the lower value of (WCA) denotes a more hydrophilic membrane surface [36]. It was perceived that the inclusion of SA in the

membrane enhanced its hydrophilicity, where the contact angle dropped from 64.9° of PSF to 61.9°, and 60.2° of PSF/PVP and PSF/SA membranes, respectively. Incorporation of SA in the membrane increased the membrane porosity from 13.5 % to 25.9 % and also improved the water uptake capacity from 11.2 % to 30.3 % (Fig. 8).

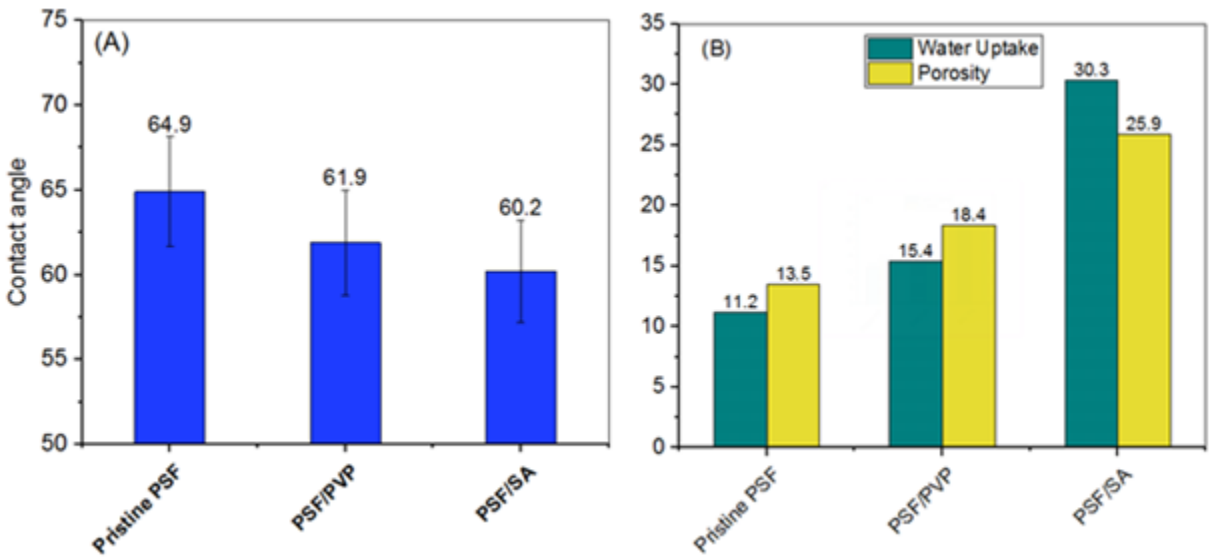


Fig. 8. Contact angle (A), Water content and Porosity (B) measurements of different PSF membranes.

3.1.4 Surface area and pore size analysis

A fully automated analyzer for BET analysis was utilized to evaluate specific surface area (SSA) of membrane samples precisely by measuring nitrogen multilayer adsorption as a function of relative pressure. The total SSA in m²g⁻¹ was determined by measuring the external area and pore area which provides a significant information on surface porosity and pore size [37]. Results exhibited in Table 2 display an increase in surface/pore

area and a decrease in the pore diameter but not obvious change in the pore volume by adding SA to the membrane polymer. The contact of water molecules with the membrane increases with increasing of membrane surface area subsequently the water permeability increases. From the results of BJH plot, the average pore diameter of SA incorporated membrane is 42.7 nm which is in the mesoporous range [38].

Table 2. Analytical results of specific surface area, pore size and pore volume of membrane samples.

Membrane type	Surface a	rea (m²g ⁻¹) BJH		ore diameter m) DFT	Pore BET	volume (cr BJH	n³g ⁻¹) DFT
Pristine PSF	2.92	5.87	67.62	41.93	0.67	0.099	0.0503
PSF/PVP	3.53	6.68	52.14	45.88	0.812	0.087	0.0506
PSF/(PVP+SA)	3.29	6.17	42.7	40.94	0.755	0.066	0.0532

3.1.5 Mechanical analysis

When a membrane is dilated (stretched), the extreme stress which the membrane can resist is known as Tensile Strength [39]. TS and elongation of membrane samples were examined. Table 3 shows the results and Fig. 9 illustrates the stress-strain curves. It can be observed from the results that TS and elongation values for TFC membranes are higher than that of their PSF support layers which indicates good mechanical properties for the

polyamide film. The SA modified membranes displayed an improvement in TS relative to the membranes modified with PVP only. The hydrogen bonding between SA and the polymer molecules besides the sponge-like structure are expected to be the reason for this enhancement since the mechanical properties rely mainly on the microstructure and intermolecular forces. The literatures [15,40] have reported (observed) a similar behavior.

Table 3. The results of mechanical analysis test of membrane samples.

Membrane type	Tensile Strength (MPA)	Elongation (%)
Pristine PSF	29.92	7.98
PSF/(PVP+SA)	30.55	3.23
PSF/PVP (TFC)	31.36	5.5
PSF/(PVP+SA) TFC	32.27	10.24

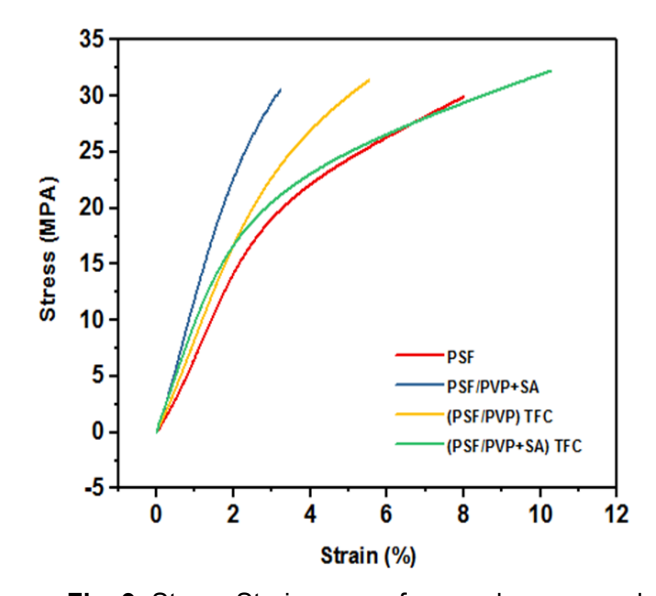


Fig. 9. Stress-Strain curves for membrane samples.

3.2 Performance study and evaluation of the fabricated NF membranes

A cross-flow unit was utilized for the evaluation of the membranes efficiency and a feed solution of 2300 ppm Na₂SO₄ was used for this purpose. The permeate flux and salt rejection for support layers containing various PSF concentrations are presented in Fig. 10A. As shown in the figure, increasing of PSF concentration leads to decreasing the permeate flux while the salt rejection increases. Increasing the polymer concentration increases the casting solution viscosity which increases the obstruction of mass movement during the phase inversion process and thereby decreases mutual diffusion between solvent in the casting solution and water in the coagulation bath leading to the formation of a dense and less porous structure with thicker The smaller pore size and porosity skin layer [41]. increases the resistance for water transport and hence decreases the permeate flux through the membrane [42]. Considering both of the permeate flux (15 L/m²h) and the salt rejection (77.7 %) results, a concentration of 16 wt. % was considered to be the optimum concentration for the used polymer. As shown from the results in Fig.10B, the permeate flux increased with increasing of PVP dosage in the casting solution which could be as a result of the increase in the porosities, pore size and surface hydrophilicity of the membrane [43]. Considering both of the permeate flux (23.1 L/m²h) and the salt rejection (91 %) results, 0.35 wt. % was considered to be the optimum concentration for the used PVP. Inclusion of SA moieties increased the membranes hydrophilicity which resulted in increasing the pure water flux with increasing the SA ratio. Similarly, the existence of polar carboxyl (-COOH) and hydroxyl (-OH) functional groups, which were brought by SA helped to capture Water molecules on the membrane surface. The results in Fig.10C indicate that the permeate flux has rised from 25.6 to 29.6 L/m²h with increasing the SA concentration from 0.08 to 0.35 wt. % . The decline in the flux at the acid concentration above (>0.35 wt.%) may due to the increment in binding force or hydrogen bonding between the acid and functional groups of the polymer molecules and thereby decreasing the free space between molecules. Subsequently, the polymer obtained membranes turn into more compact and less porous compared to the membranes prepared by lesser concentrations of acid. Also, the higher acid concentration could rise the casting solution viscosity, that could hinder the solvent (DMF) and water diffusion and exchange rate in undermost support stratum leading to the formation of a membrane of fewer porosity with more dense and thick sub-layer.

3.3. Membrane filtration efficiency at various working circumstances:

3.3.1 Influence of pressure

The impact of pressure on the membrane efficiency is illustrated in Fig. 11A. As elucidated from the results, the water flux increases by raising the applied pressure with maintaining the Na_2SO_4 salt rejection at 91.5-93 %. Increasing the pressure leads to increasing the driving force on water to be diffuse through the membrane overcoming the membrane resistance [44]. Increasing the trans-membrane pressure from 5 bar to 20 bar has resulted in increasing the permeate flux linearly from 30.4 L/m²h to 133.6 L/m²h. This linear increase is in coincidence with Fick's law, which states that transport rate varies linearly with driving force [45].

3.3.2 Influence of salt concentration

The permeate flux and salt rejection for the composite membrane with diverse salt concentrations are displayed in Fig. 11B. Four concentrations are considered in this case. ranged from 2600 to 11460 ppm. As shown in the figure, increasing the salt concentration resulted in decreasing the permeation flux. This may be because of the raise in the concentration polarization onto the membrane surface besides the increment in the solution viscosity as well. At a specific limit, the membrane pores may be blocked by the salt particles. All these possible factors may give rise to lowering the water flux [44]. Concentration polarization is a phenomenon which takes place when concentration at the membrane-liquid interface is higher than that of the bulk of solution which gives rise to an increase in osmotic pressure across the membrane and a decrease in the leading force of mass transfer. Consequently, the resistance for components transport through the membrane increases and permeation flux decreases significantly [46].

3.3.3 Influence of salt type

Fig. 11C shows that the membrane rejection of sulfate ion salts (Na_2SO_4 and $CaSO_4$) is higher than chloride ion salts ($MgCl_2$ and NaCl). This can be elucidated by the principle of Donnan's exclusion, which demonstrate that lower valence co-ion (Cl-) contributes to lower rejection of ions while lower valence counter-ion (Na-) leads to higher rejection of salts [15]. The acid modified membrane showed a salt rejection of 94.8 %, 81.5%, 24.5 %, 18.2 % and a permeate flux of 58.4, 54.4, 80, 72 L/m²h at 10 bar for Na_2SO_4 , $CaSO_4$, NaCl and $MgCl_2$ respectively.

3.3.4 Effect of operation time (Scaling study)

A solution of 2000 ppm CaSO₄ was used at 10 bar to evaluate the stability and antifouling effectiveness of the modified NF membrane. Fig. 11D shows the graph of flux

(L/m².h) versus time (hour). During the long period of filtration for CaSO₄ solution, the membrane pores are fouled and the flux is decreased. The period of filtration was about 7 hours and the amount of flux reduction was measured. The relative flux reduction (RFR) calculated for NF membrane was about 23.2 % that shows the antifouling ability of the modified membrane. RFR parameter was calculated by the following equation [47]:

RFR (%) =
$$(\frac{J_f - J_i}{I_i}) \times 100$$
 (5)

where J_f and J_i refer to the final and initial fluxes, respectively. As the RFR value is low, the antifouling property is high.

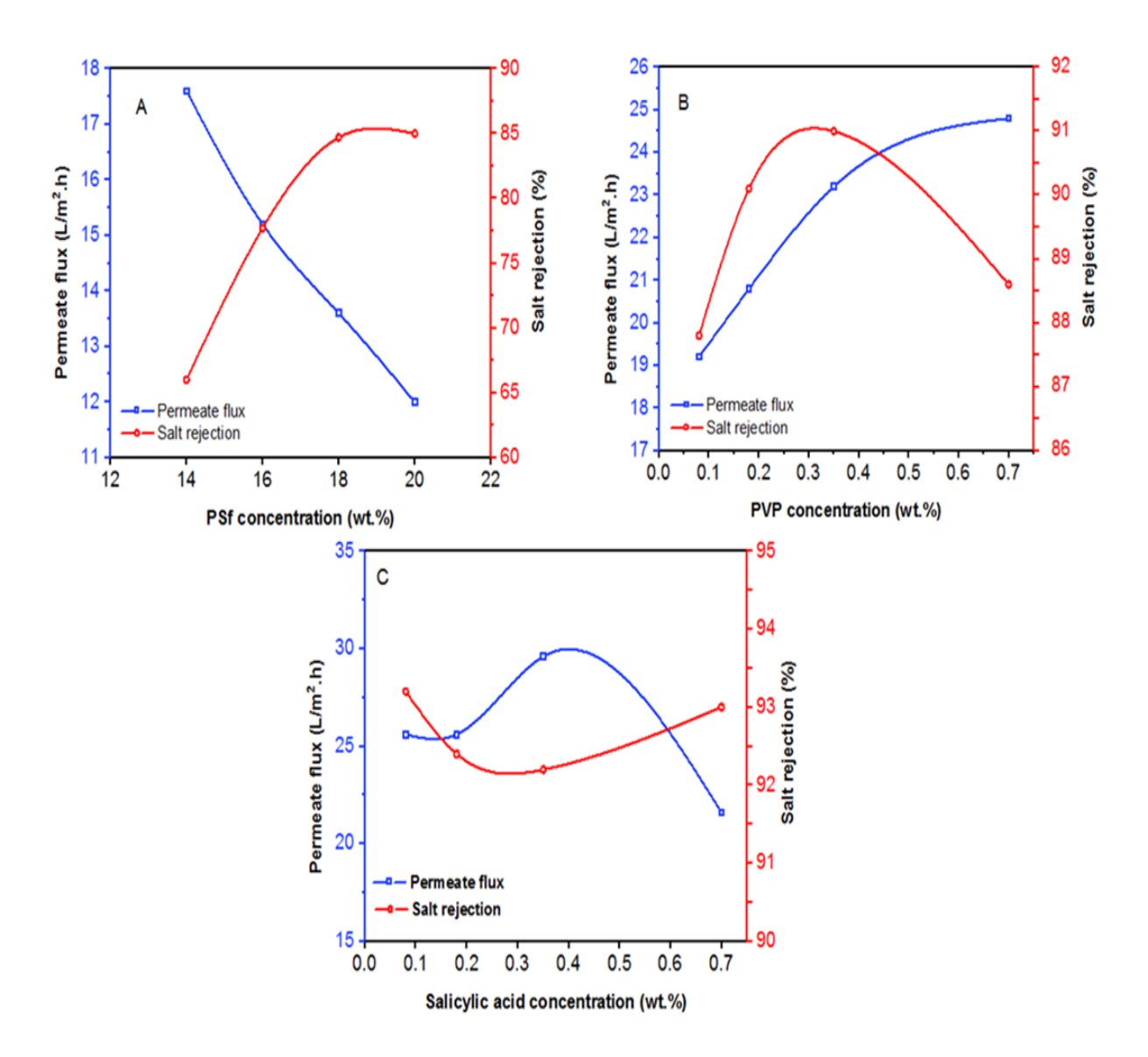


Fig. 10. Permeate flux and salt rejection of TFC membranes as a function of (A) PSF concentration, (B) PVP concentration and (C) SA concentration at Pressure 5 bar, PSF 16 % (wt/v), PVP 0.35 wt. %, PIP 1% (wt/v) for 2 min., TMC 0.15 %(wt/v) for 30 sec.

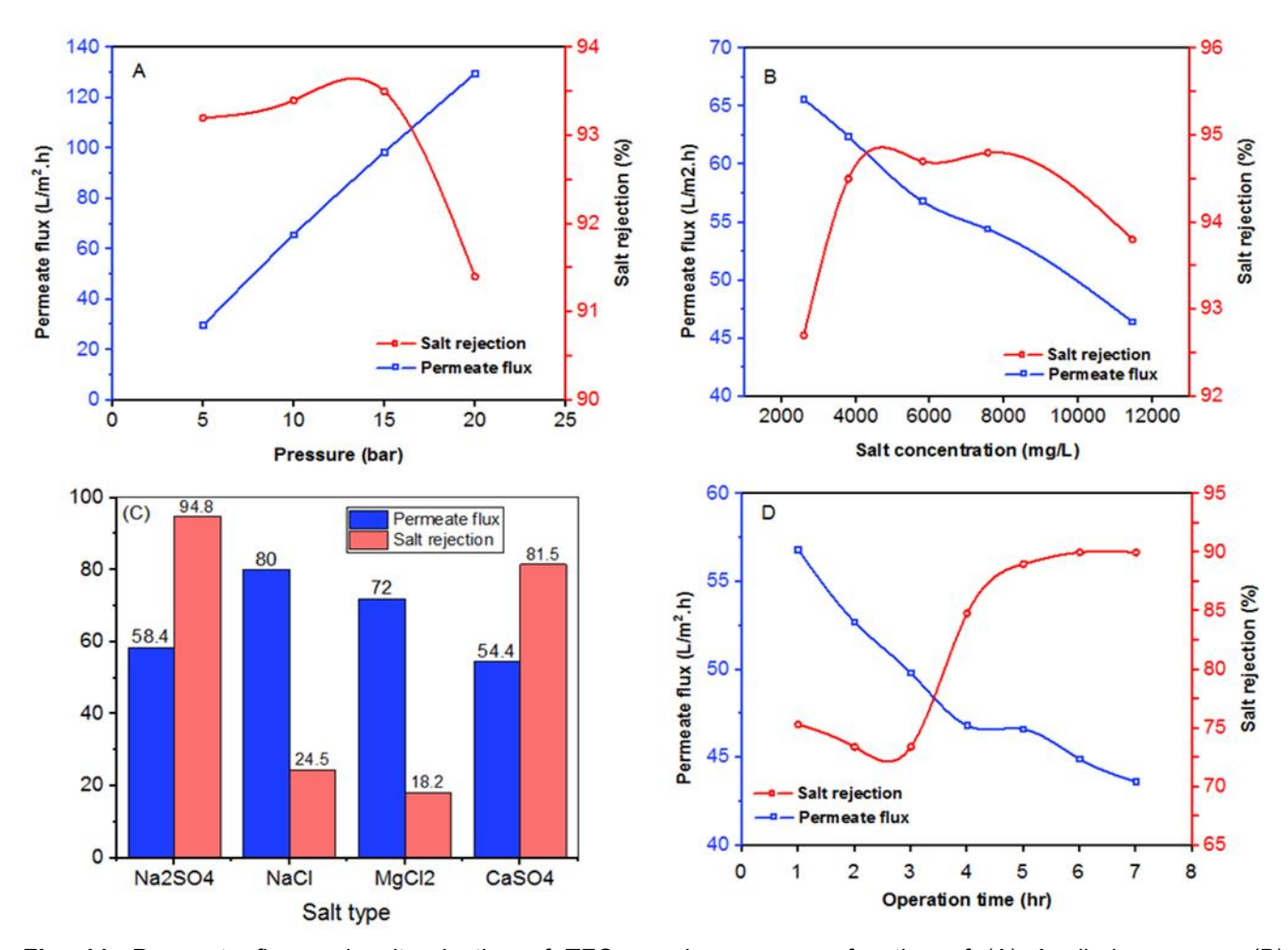


Fig. 11. Permeate flux and salt rejection of TFC membranes as a function of (A) Applied pressure, (B) Salt concentration, (C) Salt type and (D) Operation time at 2600 mg/L Na₂SO₄, Pressure 10 bar, PSF 16 % (wt/v), PVP 0.35 wt%, SA 0.35 wt%, PIP 1% (wt/v) for 2 min., TMC 0.15 %(wt/v) for 30 sec.

Conclusion

This paper investigated the effectiveness of adding PVP and SA additives in different ratios to PSF casting solution on the resulted membrane performance and structure. The effectiveness of PSF concentration was also studied. The following are the highlights of the present work:

- (I) Increasing PSF concentration decreased the resulted TFC membrane permeability which may be due to low porous support layer structure.
- (II) Addition of PVP in the PSF/DMF system increased the membrane hydrophilicity and permeability and changed the cross-sectional structure of support layer from more spongy type to more finger-like.
- (III) The surface porosity and hydrophilicity of the resulted membranes were significantly enhanced via the existence of SA in the membrane support stratum and subsequently improved the solute water flux for the fabricated TFC membranes. The results indicated that 0.28 % increase in the permeate flux of TFC/PVP membrane blended with 0.35 % SA more than that of the parallel membrane without

- SA. Also, an enhancement in the membrane surface area, tensile strength and elongation by the addition of SA.
- (IV) The optimum composition for the membrane support stratum which gives the best water permeability and salt rejection includes made over substrate of 16% PSF and 0.35% PVP with 0.35% SA.

References

- [1] Tang, C. Y.; Yang, Z.; Guo, H.; Wen, J. J.; Nghiem, L. D.; Cornelissen, E. (2018), "Potable Water Reuse through Advanced Membrane Technology", Environ. Sci. Technol. 52, 10215–10223.
- [2] Van der Bruggen, B.; Vandecasteele, C. (2002), "Distillation vs. membrane filtration: "overview of process evolutions in seawater desalination". Desalination, 143, 207–218.
- [3] M. Mulder. (1991), "Basic Principles of Membrane Technology." Dordrecht: Kluwer Academic Publishers, 1991. 360 p. ISBN (Print) 0792309790.
- [4] S.Pourjafar et al. (2012), "Synthesis and characterization of PVA/PES thin film composite nanofiltration membrane modified with ${\rm TiO_2}$ nanoparticles for better performance and surface properties", Journal of Industrial and Engineering Chemistry 18, 1398–1405.

- [5] Muneer M. Ba-Abbad et al. (2017), "Synthesis of Iron Oxide Nanoparticles to Enhance Polysulfone Ultrafiltration Membrane performance for Salt Rejection.", Chemical engineering transactions, Vol. 56.
- [6] G.L. Jadav, P.S. Singh (2009), "Synthesis of novel silicapolyamide nanocomposite membrane with enhanced properties", Journal of Membrane Science 328, 257–267.
- [7] BH Jeong, E Hoek, Y Yan, A Subramani, X Huang (2007), "Interfa- cial polymerization of thin film nanocomposites: A new concept for reverse osmosis membranes.", Journal of Membrane Science 294: 1-7.
- [8] A.K. Ghosh, E.M.V. Hoek (2009), "Impacts of support membrane structure and chemistry on polyamide–polysulfone interfacial composite membranes", J. Membr. Sci. 336, 140–148.
- [9] P.S. Singh, S.V. Joshi, J.J. Trivedi, C.V. Devmurari, A.P. Rao, P.K. Ghosh (2006), "Probing the structural variations of thin film composite RO membranes obtained by coating polyamide over polysulfone membranes of different pore dimensions.", J. Membr. Sci. 278, 19–25.
- [10] H.I. Kim, S.S. Kim (2006), "Plasma treatment of polypropylene and polysulfone supports for thin film composite reverse osmosis membrane", J. Membr. Sci. 286, 193–201.
- [11] L. Hu, S. Zhang, R. Han, X. Jian (2012), "Preparation and performance of novel thermally stable polyamide/PPENK composite nanofiltration membranes", Appl. Surf. Sci. 258, 9047–9053
- [12] G.Z. Ramon, M.C.Y. Wong, E.M.V. Hoek. (2012), "Transport through composite membrane, part 1: is there an optimal support membrane?" J. Membr. Sci. 415–416, 298–305.
- [13] C Tam, T Tweddle, O Kutowy, Hazlett (1993), "Polysulfone mem- branes II. Performance comparison of polysulfone-poly-(N-vinyl- pyrrolidone) membranes.", Desalination 89: 275-287.
- [14] C Smolders, A Reuvers, R Boom, I Wienk (1992), "Microstructures in phase-inversion membranes. Part 1. Formation of macrovoids.", Journal of Membrane Science 73: 259-275.
- [15] M.E.A. Ali et al. (2020), "Enhancing the performance of TFC nanofiltration membranes by adding organic acids in polysulfone support layer", Polymer Testing 91, 106775.
- [16] N. Ghaemi, S.S. Madaeni, A. Alizadeh, P. Daraei, M.M.S. Badieh, M. Falsafi, V. Vatanpour (2012), "Fabrication and modification of polysulfone nanofiltration membrane using organic acids: morphology, characterization and performance in removal of xenobiotics", Separ. Purif. Technol. 96, 214–228.
- [17] A. Akbari, N. Ostadmoradi, S.M.M. Rostami, M. Homayoonfal (2017), "Role of organic acids in flux enhancement of polyamide nanofiltration membranes", Chem. Eng. Technol. 40, 76–87.
- [18] G. Arthanareeswaran, D. Mohan, M. Raajenthiren (2010), "Preparation, characterization and performance studies of ultrafiltration membranes with polymeric additive", J. Membr. Sci. 350, 130–138.
- [19] P. Sherugar, N.S. Naik, M. Padaki et al. (2021), "Fabrication of zinc doped aluminium oxide/polysulfone mixed matrix membranes for enhanced antifouling property and heavy metal removal.", Chemosphere, 275, 130024.
- [20] Abdul Latif Ahmad et al. (2018), "Antifouling Properties of PES Membranes by Blending with ZnO Nanoparticles and NMP–Acetone Mixture as Solvent", Membranes, 8, 131.
- [21] Muneer M. Ba-Abbad et al. (2017), "Synthesis of Iron Oxide Nanoparticles to Enhance Polysulfone Ultrafiltration Membrane

- performance for Salt Rejection.", Chemical engineering transactions, Vol. 56.
- [22] Saleh, T.A., Gupta, V.K., (2012), "Synthesis and characterization of alumina nano-particles
- polyamide membrane with enhanced flux rejection performance.", Separation & Purification
- Technology 89, 245-251.
- [23] Solomon, M.F.J., Bhole, Y., Livingston, A.G., (2013), "High flux hydrophobic membranes for organic solvent nanofiltration (OSN)—Interfacial polymerization, surface modification and solvent activation". J MEMBRANE SCI 434, 193-203.
- [24] Yin, J., and B. Deng. (2015), "Polymer-Matrix Nanocomposite Membranes for Water Treatment". Journal of Membrane Science. 479: 256-275.
- [25] Hoan Thi Vuong Nguyen et al. (2019), "Preparation and Characterization of a Hydrophilic Polysulfone Membrane Using Graphene Oxide", Hindawi Journal of Chemistry Vol. 2019, Article ID 3164373, 10 pages https://doi.org/10.1155/3164373.
- [26] Mohd Ikmar Nizam Mohamad Isa et al. Development Cellulose-based films containing salicylic acid for wound dressing applications: fabrication, properties and in vitro assessment. Journal of Bioactive and compatible polymers 2024, Vol. 39(4) 251-263.
- [27] Trivedi MK, Branton A, Trivedi D, Shettigar H, Bairwa K, et al. (2015), "Fourier Transform Infrared and Ultraviolet-Visible Spectroscopic Characterization of Biofield Treated Salicylic Acid and Sparfloxacin". Nat Prod Chem Res 3: 186. doi:10.4172/2329-6836.1000186.
- [28] K. Meschke et al. (2018), "Characterization and performance evaluation of polymeric nanofiltration membranes for the separation of strategic elements from aqueous solutions", Journal of Membrane Science 546, 246–257.
- [29] G.L. Jadav, P.S. Singh (2009), "Synthesis of novel silica-polyamide nano-composite membrane with enhanced properties", Journal of Membrane Science 328, 257–267.
- [30] A. Mollahosseini, A. Rahimpour (2013), "Interfacially polymerized thin film nanofiltration membranes on TiO_2 coated polysulfone substrate", Journal of Industrial and Engineering Chemistry, 20 (4):1261–1268. http://dx.doi.org/10.1016/j.jiec.2013.07.002.
- [31] G.S. Lai et al. (2018), "Tailor-made thin film nanocomposite membrane incorporated with graphene oxide using novel interfacial polymerization technique for enhanced water separation", Chemical Engineering Journal 344, 524–534.
- [32] Ahmed Akbari et al. (2014), "Preparation of Novel Thin-Film Composite Nanofiltration Membranes for Separation of Amoxicillin", JNS 4, 199-210.
- [33] Febriasari, A.; Huriya; Ananto, A.H.; Suhartini, M.; Kartohardjono, S. (2021)," Polysulfone–Polyvinyl Pyrrolidone Blend Polymer Composite Membranes for Batik Industrial Wastewater Treatment.", Membranes, 11, 66. https://doi.org/10.3390/ membranes 11010066.
- [34] N. Misdan, W. Lau, A. Ismail, T. Matsuura (2013), "Formation of thin film composite nanofiltrat-ion membrane: effect of polysulfone substrate characteristics", Desalination 329, 9–18.
- [36] P.Veerababu et al (2014), "Limiting thickness of polyamide—polysulfone thin-film-composite nanofiltration membrane / Desalination 346, 19–29.
- [37] B.S. Mbuli et al. Polysulfone Ultrafiltration Membranes Modified with Carbon-Coated Alumina Supported Ni-TiO₂ Nanoparticles for Water Treatment: Synthesis, Characterization

- and Application Journal of Membrane Science and Research 5 (2019) 222-232.
- [38] Galal A M Nawwar et.al. (2022), "Utility of a New Non-Toxic Antibacterial Cellulose Membrane Prepared via Casting Technique.", Egypt. J. Chem. Vol. 65, No. 3 pp. 73 79.
- [39] Nhlengethwa, S.T; Tshangana, C.S.; Mamba, B.B Muleja, A.A. (2024), "The Application of TiO₂/ZrO₂-Modified Nanocomposite PES Membrane for Improved Permeability of Textile Dye in Water.", Membranes 14, 222. https://doi.org/10.3390/membranes14100222.
- [40] Alosaimi, A.M. (2021), Polysulfone Membranes Based Hybrid Nanocomposites for the Adsorptive Removal of Hg (II) Ions. Polymers 13, 2792. https://doi.org/10.3390/polym13162792.
- [41] Zhen Liu et al. (2015), "Preparation and Performance of Sulfonated Polysulfone Flat Ultrafiltration Membranes", Polymer Engineering and Science. Society of Plastics Engineers 2014. 55 (5): 1003-1011. DOI 10.1002/pen. wileyonlinelibrary.com
- [42] Liu Z., Bai Y., Sun D, C., Xiao A., Zhang 10. Y. (2014), "Preparation and Performance of Sulfonated Polysulfone Flat Ultrafiltration Membranes", Polym. Eng. Sci. 55, 1003-1011.

- [43] Baolin Deng (2014), "Effects of Polysulfone (PSf) Support Layer on the Performance of Thin-Film Composite (TFC) Membranes", J Chem Proc Eng 1: 1-8.
- [44] A.E. Abdelhamid et al. Polysulfone nanofiltration membranes enriched with functionalized graphene oxide for dye removal from wastewater. J Polym Eng 2020; 40(10): 833–841. https://doi.org/10.1515/polyeng-2020-0141
- [45] Jayant S et al. (2016(, "Polysulfone based Ultrafiltration Membrane Preparation by Phase Inversion: Parameter Optimization.", International Journal of Science and Research (IJSR). Volume 5 Issue 6.
- [46] A. Shahtalebi et al. (2011), "Application of nanofiltration membrane in the separation of Amoxicillin from pharmaceutical wastewater" Iran. J. Environ. Health. Sci. Eng. Vol. 8, No. 2, pp. 109-116.
- [47] N. Shaabani, S. Zinadini, A.A. Zinatizadeh (2018), "Preparation and characterization of PES nanofiltration membrane embedded with modified graphene oxide for dye removal from algal wastewater", Journal of Applied Research in Water and Wastewater, 5 (1), 407-410.